GENETIC ALGORITHM APPLIED TO A FORCED LANDING MANOEEUVRE

Peter Tong*, Cees Bil** George Galanis[‡]
*[†]RMIT University, [‡]Defence science and Technology Organisation Australia

Keywords: *genetic algorithm, forced landing, flight paths*

Abstract

In this research a trajectory optimisation was being undertaken using Genetic Algorithm to search for optimal landing manoeuvres for a forced landing of an airplane after engine failure using a simplified analytical model for the Beech Bonanza model E33A retractable-undercarriage aircraft. Vertical atmospheric disturbances were simulated using an approximated von Karman low altitude model for the atmospheric disturbance model based on the MIL-F-8785C specifications. A forced landing manoeuvre analysis was carried out for an engine failure at 650 ft AGL for bank angle varying from banking left at 45° to banking right at 45° and with an aircraft's speed varying from 75.6 mph to 208 mph corresponding to 5% above airplane's stall speed and airplane's maximum speed respectively. The results show the effects vertical disturbances have on the general flight paths for three pre-selected landing locations.

1 Introduction

The study of safe landing of aeroplanes is a very important issue in the aviation field and is considered by pilots as the most demanding task in every flight. Many accidents have occurred during the landing phase of flights, some of which were beyond the pilot's control, some were due to human error, while some could have been successful if only a more optimal landing manoeuvre was carried out. Unfortunately, it is the disastrous failed landings that became a statistics with the National Transportation Safety Board (NTSB) and those who landed safely or with minor damage generally are not reported to Federal Aviation Authority (FAA) or NTSB. Hence, the statistics gathered are skewed or biased towards failed attempts.

The research problem in this study has its interest in the search for the best landing trajectory for a forced landing manoeuvre of an aircraft after an engine failure. Such situation could occur after take-off [1] or during a level flight at any altitude above ground level (AGL) [2]. When an engine failure occurs in an aircraft and no additional power is available, the pilot must select a suitable location to land safely with the limited amount of energy available from the engine failure position. The general recommendation is to land straight ahead and Rogers' studies [1] confirmed the high rates of using this ingrained technique. However, he suggests that, for forced landings from a higher altitude, a turnback manoeuvre may be flown because higher altitude allows for more time in the air. This research is also an extension of Rogers' forced landing manoeuvre where the search for optimal landing paths begins after the pilot has selected a practical landing location on the ground that is within range after an engine failure. A study on the effects vertical atmospheric disturbances have on a forced landing manoeuvre was also carried out.

2 Problem Description – Forced Landings

Landing an aircraft that has suffered an engine failure during take-off is one of the classifications of a forced landing and is the focus of this study. The general recommendation in the aviation literature for such a situation is to land straight ahead [3, 4]. For example, FAA regulations recommend that pilots land straight ahead and should never attempt track reversals in an effort to land on the departure runway. The present research problem is an extension of a forced landing manoeuvre on the Beech E33A Bonanza single engine aircraft considered by Tong, Galanis and Bil[5] based on Rogers[1]. The problem considered in this forced landing assumed an engine failure at 650 ft AGL after take-off. It used the engine failure point as the reference point for all distances calculated. It was assumed that the transition in speed occurred instantaneously and the effects of landing gear retraction/extension were not considered.

A graphical interpretation of the forced landing after an engine failure at an arbitrary altitude is shown in Fig. 1. This research took the approach of an ensemble of probability of landing within a specified tolerance from a pre-selected location and not as an optimal control problem of the deviation from the flight trajectory during a forced landing manoeuvre. In other words, what are the chances of the pilot performing the landing task with maximum probability of landing on a pre-selected landing site? The calculations performed in this study used the general flight dynamics equations [6] and data based on the Beech Bonanza E33A retractable aircraft characteristics obtained from Rogers as shown in Table 1. The data for initial takeoff ground roll and distance to clear 50 ft obstacle are obtained from Rising Up Aviation Resources[1].

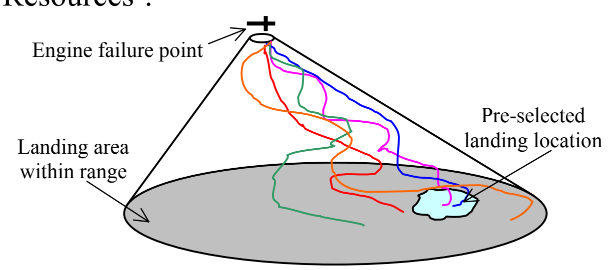

Fig. 1. Forced Landing Area

[1] Data available online at http://www.risingup.com/planespecs/info/airplane117.shtml. 2003.

Table 1. Beech Bonanza Model 33A characteristics [1]

Parameter	Value
Gross Weight, lb	3300
Wing Area, ft^2	181
L/D_{max}	10.56
Power, brake horsepower	285
Propeller	Constant speed 3-blade
V_{max}, mph	208
V_{cruise} at 65%, mph	190
$V_{stall(clean)}{}^{a}$ power off, mph	72
$V_{stall(dirty)}$ power off, mph	61
$V_{L/Dmax}{}^{b}$, mph	122
$V_{\gamma max}{}^{c}$ at sea level, mph	91
$V_{R/Cmax}{}^{d}$ at sea level, mph	112.5
R/C at sea level and 3300 lb, ft/min	1200
Parabolic drag polar	$C_D = 0.019 + 0.0917C_L^2$
Takeoff: Ground roll, ft	880
Takeoff: Over 50 ft obstacle, ft	1225
Landing: Ground roll, ft	625
Landing: Over 50 ft obstacle, ft	1150

[a] Gear and flaps retracted.
[b] L/D_{max} = maximum lift to drag ratio.
[c] γ = glide angle.
[d] R/C_{max} = maximum rate of climb.

3 Atmospheric Model

The simulation of atmospheric turbulence is of considerable importance and is a critical component in any aircraft simulation and in trajectory optimisation development. Atmospheric disturbances are very random by nature and so are its magnitudes and the frequencies of occurrence. They are affected, for example, by the geographical location, the weather and the time of the year.

For this study, the von Karman low altitude model and the medium altitude model for atmospheric disturbance model based on the MIL-F-8785C specifications were used to simulate the atmospheric turbulence model [7]. The atmospheric turbulence velocity for this research was calculated using [8]'s approximated transfer function from the von Karman spectrum.

The vertical turbulence velocity terms were vectorially added to the aircraft's velocity and were assumed to have an instantaneous change to the aircraft's vertical velocity. The aircraft was also assumed to be flying through a one-dimensional gust field where only the vertical velocity changed and it was assumed that the turbulence encountered was independent of time. In other words, the turbulence profile was frozen or fixed in space and time.

The influence of wind velocities have on an aircraft could be roughly separated into 2 parts. The flight performance description of an aircraft depends on the low frequency part of the wind vector, the wind shear component. It is only the low frequency part of the wind that influences the energy relation of the aircraft. The high frequency wind components in the atmospheric turbulence and gust are considered high frequency and have no effect on the aircraft trajectory. Their effects are on the aircraft's loading, the structural fatigue, the pilot's workload, passenger comfort, and on the flying qualities of the aircraft. The eigenmotions of the aircraft, the phugoid and the short period motion are important frequencies for the separation effects. If the frequency of the wind perturbation is less than the phugoid frequency, the change of aircraft trajectory is directly proportional to the wind angle of attack, meaning the low frequency directly changes the aircraft trajectory. If the range of frequency is above the short period motion, the inertia of the aircraft avoids large change of trajectory. In other words the flight path is only affected in phugoid mode where the pitch angle follows the flight path angle [9-11]. Using the airplane's stall speed (V_s = 72 mph) and the well-known phugoid period equation, the phugoid period was found to be $T_{Phugoid} = \frac{\sqrt{2}\pi V}{g} \approx 15\,\text{sec}$.

100 atmospheric turbulence profiles were generated for reference speed of 15 kts at 650 ft AGL using the von Karman atmospheric turbulence model. An improvisation to the atmospheric turbulence model was made by time averaging the von Karman atmospheric turbulence model to coincide with the airplane's approximated phugoid mode of 15 secs. This in effect is one method of obtaining the low frequency velocity representations. The maximum time averaged atmospheric turbulence updraft is 1.48 ft/sec and the maximum downdraft is –1.67 ft/sec.

4 Genetic Algorithms

Drawing parallels from natural selection, Holland[12] proposed the theory of GA in the early 1970's which imitates the evolutionary processes in nature. Evolution can be considered as a form of an optimisation problem where only the fittest individuals will survive and reproduce, also known as the "survival of the fittest". GAs use crossovers – a probabilistic mechanism for randomising chromosomes, and mutations – a perturbation mechanism, as search mechanisms to generate a sequence of populations. The most rudimentary unit, the genes, which can take the form of different alleles, are combined to form chromosomes that control the "keys" to the survival of the individual in a competitive environment. Evolution occurs when the chromosomes from two parents are combined during reproduction and a new gene pool is formed from combinations generated through either crossover or mutation.

GAs perform parallel, non-comprehensive search in the hope of finding the global maximum, if not a very near optimal solution, to optimisation problems. The procedure to solve a complex problem using GAs is to define the search space and to custom design a coding scheme for the solutions in the search space tailored to the problem. This process is known as genetic representation[13]. A fitness function is then designed to evaluate the potential solutions, and the "better" ones are kept for subsequent regenerations and the "inferior" solutions are discarded. The next generation of solutions are created by applying the crossovers and mutations genetic operators to evolve solutions for further fitness evaluations. The optimisation process terminates when either an acceptable tolerance in results is obtained, or when it has processed a specific number of generations, or when no improvement in fitness value is encountered after a number of consecutive generations. The GA cycle is shown in Fig. 2. The three most important features are fitness function, the genetic encoding and the genetic operators.

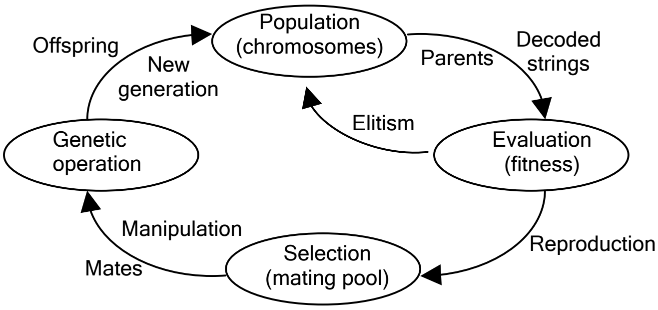

Fig. 2. Genetic Algorithm Cycle

GA is a relatively new optimisation method compared to the traditional gradient search method, which has difficulties for discontinuous or non-smooth functions. In solving optimisation problems, GAs have the advantage that no derivatives have to be found but they have only to utilize the governing equations in the problem considered. The trade off in not using gradient information is that it does not guarantee a minimum point but will locate results that are very close to the optimal solution. Other optimisation methods such as gradient method may be able to locate better optimal solutions but may suffer computational time. GA is not an alternative nor is it a replacement method to other traditional optimisation methods but it is a valid complementary optimisation technique. In simulation, obtaining acceptable results rapidly is more valuable than spending an enormous time searching for the optimal point and GA is capable of doing so.

4.1 Real-Value GA Operators

A real-value representation was used since it helped to exploit the numerical properties of a candidate solution by exploiting the solution gradients and information from the function's landscape. The GA real-value chromosomes are represented by a vector $\vec{x} = (x_{1, \dots} x_n)$, where n is the chromosome length. The chromosome length is equivalent to the number of variables used to represent the domain. Each gene, (x_k), in the chromosome is bounded by an upper limit (x_{max}) and a lower limit (x_{min}) specific to the gene.

A brief description from Michalewicz[14] is presented here for the different operators used for a real value encoding. The genetic operators used for real value encoding in this analysis consist of three types of mutation operators and three types of crossover operators:

i) ***Uniform mutation*** randomly mutates a gene in the chromosome with uniform probability distribution to any value within the real-valued domain range. This operator is important in the early phases of the evolution process, as the solutions are free to move within the search space.
ii) ***Boundary mutation*** mutates a gene to either the lower boundary value or the upper boundary value for the real-valued range. This operator is very useful for GAs with constraints.
iii) ***Non-uniform mutation*** mutates a gene by a factor that is a function of the difference in value between that particular gene and either of its boundary value, and the generation number. This mutation probability will decrease to 0 as the generation number increases. This type of mutation is used for local fine-tuning of genes where the operator will initially search the space uniformly and very locally at later generations.
iv) ***Arithmetic crossover*** linearly combines the genes from two parents to produce two children.
v) ***Simple crossover*** randomly selects a point in a chromosome as a crossover point which is very similar to the traditional one-point crossover.
vi) ***Heuristic crossover*** uses the values of the objective function to determine the direction of the search and it may or may not produce an offspring. It is responsible for local fine-tuning and search in the promising direction.

All of the six genetic operators described were required to explore the search space adequately and were used equally to prevent premature convergent without regard to fitness. For example, arithmetical crossover would tend to drive the population to the numerical center of the search space very quickly, regardless if it yields good fitness values, and boundary mutation would set the gene to either of its boundary value. However, the use of other operators will prevent such problem. It is through the combination of these powerful crossover and mutation operators developed by Michalewicz that the search space can be explored and good genetic material exploited. In order to randomise the use of the three types of crossovers and mutations uniformly, the populations were randomly chosen for the different types of crossovers and mutations. The three types of crossovers and mutations were applied equally to all the randomised populations in every generation to allow equal distribution of genetic operators.

The GA in this analysis used tournament selection, whereby two chromosomes were selected from the population and compared at any one time to select the fitter chromosome for crossover and mutation. This selection method prevented fitness scaling where a few highly fit chromosomes may dominate the parent population. It also used elitism where a certain number of the best chromosomes from the previous generation are cloned to the present generation.

4.2 Real-Value Control Parameters Selection

A common issue that arises in using GA is the proper selection of parameter settings [15-18]. Using a large population of chromosomes will increase computational time but it will prevent premature convergence to a local optimum while using a small population of chromosomes will reduce computational time but it may converge prematurely to a sub optimal solution. In general, a high crossover rate increases the recombination of building structures but an excessive crossover rate may lead to high-performance structures being discarded faster than the selection process is able produce improvement while a low crossover rate may stagnate the optimisation process. The selection of the crossover rate also depends on the population sizes where higher crossover rate for smaller populations can prevent premature convergence while lower crossover rate be used for larger populations since they have larger search space. A high mutation rate, which is more important in later generations, resembles a random search but it may help to reintroduce lost structure while a low mutation rate may lead to a convergence to a local optimum.

Since the GAs method relies on stochastic processes and is optimisation objective dependent, a control parameter test was carried out to determine the best selection of population size, the number of generations, the crossover rate and the mutation rate for the optimisation problem considered in this study. A chromosome length (l) of 26 bits, corresponding to two variables, speed and bank angle, for each of the 13 discrete altitude steps to ground level for an engine failure at 650 ft AGL was used. A genetic control parameter selection process as shown in Table 2 was carried out for three sets of pre-selected touchdown locations. They were located at 0 ft laterally and –3100 ft longitudinally, at 3000 ft laterally and 3000 ft longitudinally, and at 500 ft longitudinally and 200 ft laterally from the engine failure point with reference to the airplane's heading direction at that instance. The code for implementation of the GA was developed in Matlab 5.3. The fitness value in this GA trajectory optimisation was defined as the distance between the touchdown location and the pre-selected touchdown location.

Table 2. Real-Valued Control Parameters Selection

GA Control Parameters	Range	Step Size	Cumulative runs
Coef. for non-uniform mutation (b)	2 – 8	2	4
Crossover rate	30% – 40%	10%	8
Population size (N)	52 – 260	52	40
Mutation rate	1% – 9%	2%	200
Repetition for each test	100	1	20000

The GA control parameter selection was carried out for an elitism of 10% of the population size for subsequent generations. A larger percentage of elitism used may stagnate the evolution process while a smaller percentage of elitism used may slow down the convergence. A stopping criterion of 100 generations and a repetition of 100 GA runs were carried out for each of the 200 combinations of parameters for each test location to reduce the effect of probabilistic “noise”. For each run, the best fitness value was recorded as measure for the GA’s performance. These values were averaged over 100 runs for every combination of population sizes (N), crossover rates, coefficients for non-uniform mutation (b) and mutation rates to provide a representative performance of a general GA run. The computation cost is defined as a product of the population size and the minimum number of generations it takes to obtain the minimum fitness value for each trial limited to the stopping criterion of 100 generations used. The average performance values for each set were normalised with respect to those values from runs with population size of 52 ($2l$) and mutation rate of 1%.

Calculations were carried out using altitude steps of 50 ft for convenience instead of constant time interval steps. The reason for not using constant time interval was the requirement to terminate the GA search at exactly 0 ft AGL. In this forced landing simulation, at every 50 ft drop in altitude, the pilot continuously decides on the flying speed and bank angle. At each altitude step, the pilot may elect to turn by banking continuously at ±45 deg flying with speed varying continuously from 5% above stall speed (75.6 mph) to maximum speed (208 mph).

4.3 Results for Real-value Control Parameters Selection

Since similar trends in results were observed for all the three pre-selected touchdown locations, remarks will be made for the pre-selected location of touching down at 0 ft laterally and –3100 ft longitudinally. Larger population sizes usually provide a more accurate solution. However, for mutation rates of less than 5%, there is relatively little improvement in the fitness value for population size above $4l$ (N = 104) as shown in Fig. 3 and fitter values were obtained using a crossover rate of 30% as shown in Fig. 4 This minimal improvement in fitness value is at the expense of greater computational cost, which in general is a linear increase of computational effort for an increase in population size. While there is minimal improvement in the best fitness for populations greater than $4l$, the computational effort continues to increase as shown in Fig. 5. Hence, increasing the population size beyond $4l$ did not appear to be worth the related computational cost. The results suggest that a population size of $4l$ (N = 104) is an appropriate compromise for a best fitness value and a reasonable computational effort which agrees well with Williams and Crossley[18]. A coefficient for non-uniform mutation of 4 provided a fitter and more consistent best fitness value for the different control parameter combinations tested. Very similar results for computational cost were observed for mutation rates ranging from 3% to 9%. Nevertheless, the fitness values for these mutation rates are not as fit as the fitness value for a mutation rate of 1%. The deterioration in fitness value may be due to excessive increase of mutation in the chromosomes. Mutation rates have a significant effect on the fitness performance but its effect is reduced as the population size increase beyond $4l$.

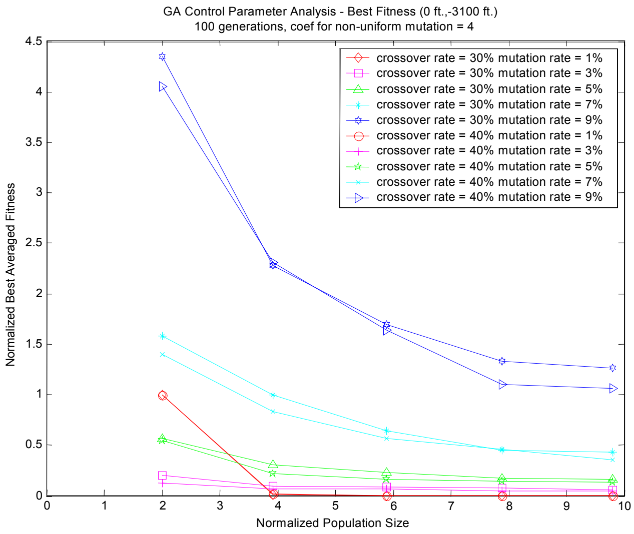

Fig. 3. GA Control Parameter – Normalised Best Fitness

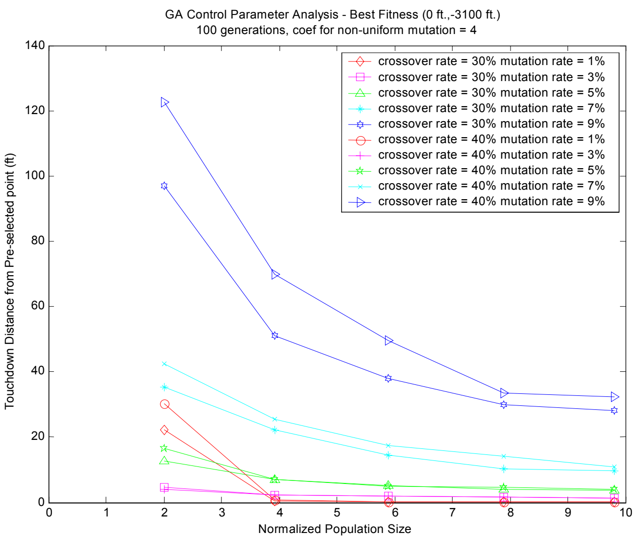

Fig. 4. GA Control Parameter – Best Fitness

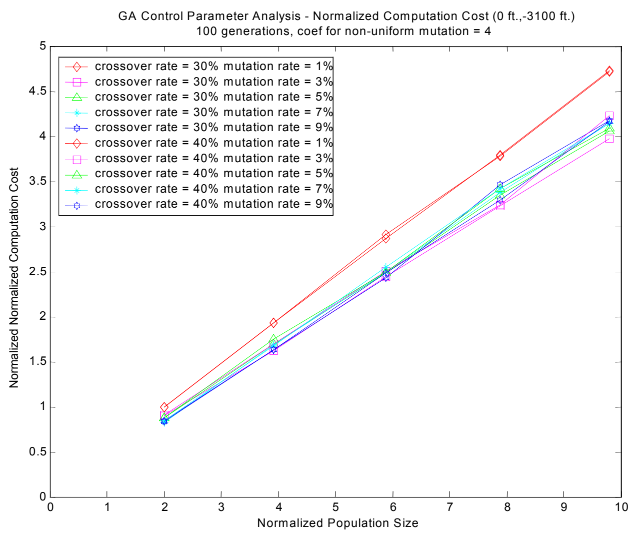

Fig. 5. GA Control Parameter Analysis – Computation Cost

Based on the GA parameter analysis carried out, a set of parameters were found suitable for further work on this particular trajectory optimisation for a forced landing manoeuvre upon engine failure. These are a population size of 104, a crossover rate of 30%, a mutation rate of 1%, a coefficient for non-uniform mutation of 4, using tournament selection and an elitism of 10% based on population.

GA convergence history is important to the understanding of its behaviour to ensure sufficient number of generations was run to obtain satisfactory results. Fig. 6 illustrates a typical convergence history for 100 generations for each of the 100 trials obtained from the control parameter selection analysis. No premature convergence was observed and the selected generation of 100 has allowed a satisfactory development of the population.

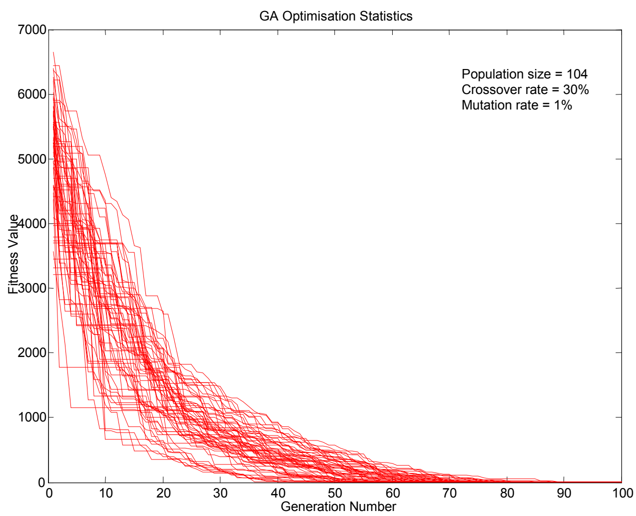

Fig. 6. Evolution History for 100 Trials

5 Results for GA in Forced Landings with Continuous Speed and Continuous Bank Angle

A GA for forced landing with continuous speed and continuous bank angle was carried out for three test locations; (0 ft, -3100 ft), (3000 ft, 3000 ft) and at (500 ft, 200 ft), where the 1st component represents the lateral distance and the 2nd component represents the longitudinal distance from the failure point. It used real-value representation and the control parameters determined in the previous section. In order to test the validity and the reliability of the real-value representation GA search procedure developed, the results were compared to the results obtained using the exhaustive search method and similar results were obtained.

5.1 Results with Still Air Conditions

The results for GA with continuous speed and continuous bank angle for touchdown distances from the respective pre-selected landing locations are shown in Table 3.

Table 3. Results for GA with Continuous Speed and Continuous Bank Angle

Pre-selected Location	Global Minimum Distance	Average Minimum Distance from 100 trials	Probability of Landing ≤ Average Minimum Distance from 100 trials
(0 ft, -3100 ft)	0.0064 ft	0.4252 ft	91 %
(3000 ft, 3000 ft)	0.0005 ft	0.0312 ft	59 %
(500 ft, 200 ft)	0.0022 ft	0.0426 ft	73 %

Based on the results obtained, the GA with continuous speed and continuous bank angle search method has successfully found suitable combinations of aircraft speed and bank angle to land extremely close to the pre-selected locations with high probability for landing within the average minimum distance except for the (3000 ft, 3000 ft) location. The lower probability in obtaining paths within the average minimum distance for location (3000 ft, 3000 ft) is due to the nature of the solution landscape. For minimum global values with neighbourhood values of very small differences, as illustrated by this particular test location, GA will have a lower probability (59%) in locating paths that are within the average minimum distance since GA concentrates in that solution space and nearby adjacent values maybe found instead. A slightly higher mutation rate may assist in locating the global minimum value better in such a solution landscape but it is not necessary since the average minimum distance from the pre-selected location is very small (0.0312 ft) for this particular location. The quality in the results obtained for all the three pre-selected locations can be observed from the probability ranging from 59% to 91% in landing less than or equal to the average minimum distance from the 100 trials.

Two general flight paths for the pre-selected location (0 ft, -3100 ft) exist since this location is located along the airplane's line of symmetry at failure point. The best flight paths found from each of the 100 runs and their average motion variables for turning right are shown in Fig.7. The results show that in order to land at the pre-selected location with high probability, the pilot flies the following manoeuvre. Upon engine failure point at 650 ft AGL, the pilot begins a tight turn either by banking steeply right or left at approximately 40° while flying at 76 mph. This is followed by increasing the airplane's speed towards 107 mph and widening of the turn radius by gradually reducing the bank angle to 23° as it descends to approximately 200 ft AGL. The pilot then continues flying at approximately 106 mph while further reducing the bank angle towards 0° until touchdown.

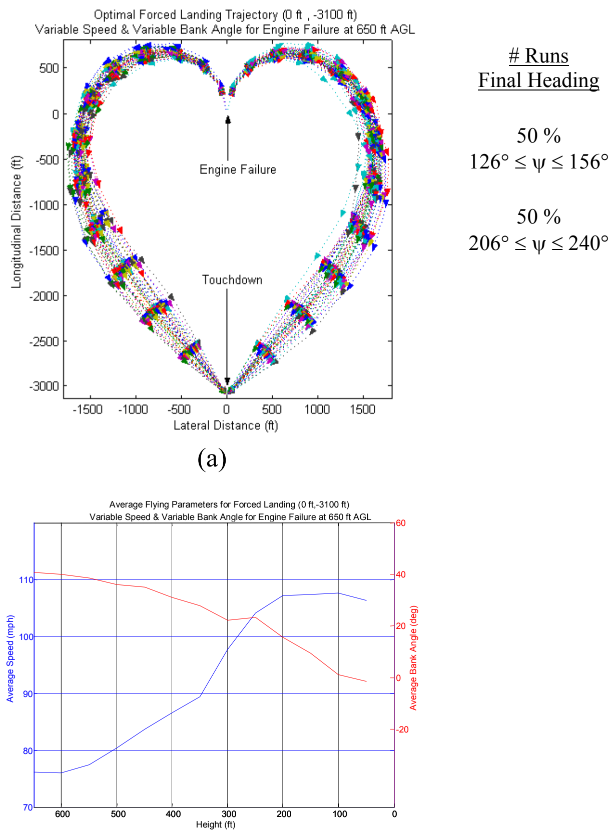

(a)

(b)

Fig. 7. Optimal Forced Landing (0 ft, -3100 ft) Continuous Speed and Continuous Bank Angle at 650 ft AGL

The best flight paths found from each of the 100 runs and their average motion variables for the pre-selected location (3000 ft, 3000 ft) are shown in Fig. 8. The general flying manoeuvre to land at the pre-selected location of (3000 ft, 3000 ft) is, upon engine failure at 650 ft AGL, to begin with a left bank of approximately 9° at 96 mph. This is followed by a right bank until approximately 15° at 500 ft AGL and a further right bank towards 22° while gradually decreasing the airplane's speed until approximately 87 mph at 250 ft AGL. The pilot then increases the airplane's speed to approximately 91 mph along with a gradual decrease in right bank angle towards 7° until touchdown. The landing manoeuvre for this pre-selected location resembles the 90° landing approach in general aviation for flying from the base leg to the final leg where the pilot begins to turn towards the pre-selected location when it is at 45° from the current position. The results also show the double base leg flight paths where at engine failure point the aeroplane turns right and then followed by a left turn to touchdown. Although these are feasible flight paths, they are generally not recommended since they are harder to fly and will cause an increase in the pilot's workload.

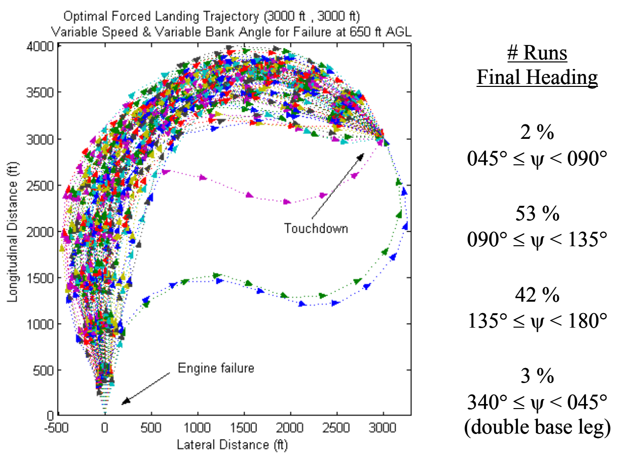

(a)

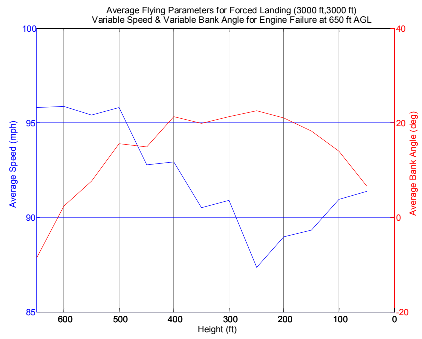

(b)

Fig. 8. Optimal Forced Landing (3000 ft, 3000 ft) Continuous Speed and Continuous Bank Angle at 650 ft AGL

The majority of the initial flight paths for the pre-selected location (500 ft, 200 ft) show that 95% of the flight paths turn toward the pre-selected location while counter intuitive flight paths of 5% turn away from the pre-selected location. The counter intuitive manoeuvre is also possible since the pre-selected location is located near the airplane's line of symmetry at engine failure point. The best flight paths found from each of the 100 runs and their average motion variables for both right and left turns for the pre-selected location (500 ft, 200 ft) are shown in Fig. 9-a. The general flying manoeuvre to land at the pre-selected location of (500 ft, 200 ft) for the turn towards the pre-selected location (see Fig. 9-b) is, upon engine failure, to fly at 100 mph, banking left at approximately 7%, then gradually decreasing the airplane's speed to approximately 79 mph while increasing the right bank angle towards 37° until 350 ft AGL. The pilot then maintains the flying speed at 79 mph while maintaining the bank angle at 37° until 250 ft AGL. This is followed by gradually increasing the airplane's speed towards 96 mph and decreasing the bank angle towards 12° until touchdown. The general flying manoeuvre for the counter intuitive manoeuvre (see Fig. 9-c) is to fly at 96 mph, banking left at approximately 5.5%, gradually decreasing the airplane's speed to approximately 77 mph while increasing the left bank angle towards 37° until 550 ft AGL. The pilot then maintains the flying speed at 75 mph while maintaining the left bank angle at 40°

until 250 ft AGL. This is followed by gradually increasing the airplane's speed towards 100 mph and decreasing the left bank angle towards 21° until touchdown. The landing manoeuvre for both manoeuvres for this pre-selected location resemble the 180° and 270° landing approach in general aviation in flying from the base leg to the final leg where the pilot begins to turn towards the pre-selected location when the pilot is abreast with the pre-selected landing location.

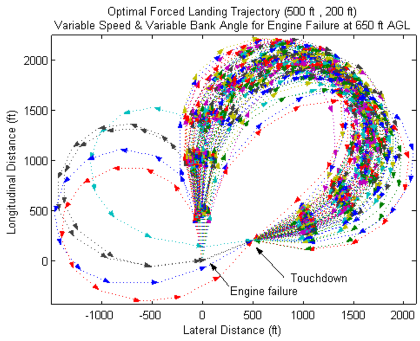

Runs
Final Heading

5 %
032° ≤ ψ ≤ 073°

95%
222° ≤ ψ ≤ 288°

(a)

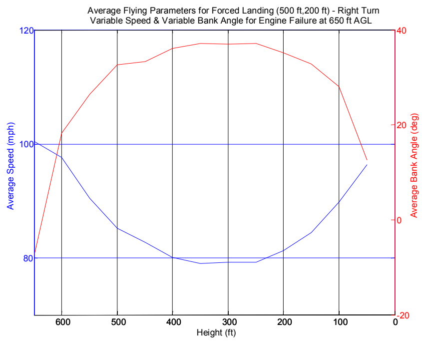

(b)

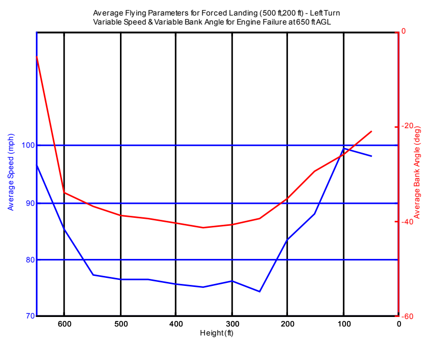

(c)

Fig. 9. Optimal Forced Landing (500 ft, 200 ft) Continuous Speed and Continuous Bank Angle at 650 ft AGL

5.2 Results with Time Averaged Vertical Atmospheric Turbulence

The results for the GA with continuous speed and continuous bank angle, and with vertical atmospheric turbulence for touchdown distance from the respective pre-selected landing locations are shown in Table 4.

The best landing flight paths from each of the 100 atmospheric turbulence profiles as shown in Fig. 10 – 12 trace a slightly wider landing flight path envelope than in still air condition. The average flying parameters with vertical atmospheric turbulence for all the three pre-selected locations are very similar to the still air condition since the disturbance is mild.

The results show that the GA with continuous speed and continuous bank angle method, and with vertical atmospheric turbulence has successfully found suitable combinations of the aeroplane's speed and bank angle to land very close to the pre-selected locations. The GA with vertical atmospheric turbulence found very minute global minimum distance from each of the three pre-selected locations. Comparatively, the average touchdown distances from all the pre-selected locations with vertical atmospheric turbulence are farther than in still air condition. This is as expected since vertical atmospheric turbulence is a form of disturbances and uncertainties to the flying manoeuvre. A very high probability (93%) of landing within the average minimum distance from the 10,000 trials was obtained for the pre-selected location (0 ft, -3100 ft) but a relatively low probability (61%) was obtained for the pre-selected location (3000 ft, 3000 ft) because GA concentrated in that solution space nearby where adjacent values were found instead.

Fig. 10-a shows the best forced landing flight paths with vertical atmospheric turbulence from each of the 100 turbulence profiles runs for the pre-selected location (0 ft, -3100 ft). Two general forced landing paths exist since the pre-selected location is located along the airplane's line of symmetry at engine failure point. The aeroplane's average flying speed and bank angle at each 50 ft decrement in altitude, and the airplane's final heading statistics to land at the

Table 4. Results for GA with Continuous Speed and Continuous Bank Angle, and Vertical Atmospheric Turbulence

Pre-selected Location	Global Minimum Distance	Average of the Minimum Distance from each Turbulence Profile	Average Minimum Distance from 10,000 trials	Probability of Landing ≤ Average Minimum Distance from 10,000 trials
(0 ft, -3100 ft)	1.4847×10^{-4} ft	0.0123 ft	0.7244 ft	93 %
(3000 ft, 3000 ft)	9.2037×10^{-4} ft	0.0045 ft	0.0625 ft	61 %
(500 ft, 200 ft)	1.4374×10^{-4} ft	0.0044 ft	0.0718 ft	70 %

pre-selected location are shown in Fig. 10-b. The results show that strong continuous downdrafts during both the turn glide manoeuvre and the straight glide manoeuvre will have the most effect in an attempt to land close to this pre-selected location. Downdrafts affect the straight glide manoeuvre more than the turn glide manoeuvre in an attempt to land close to the pre-selected location while updrafts will increase the probability of landing closer to the pre-selected location.

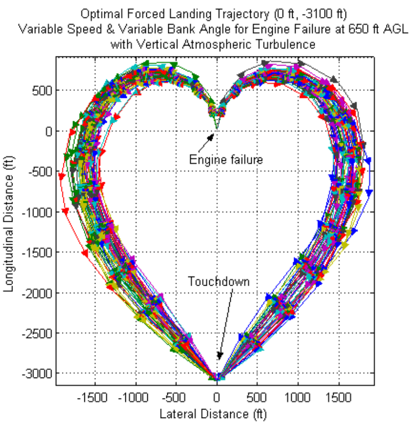

(a)

<u># Runs</u>
<u>Final Heading</u>

58 %
122° ≤ ψ ≤ 154°

42 %
201° ≤ ψ ≤ 237°

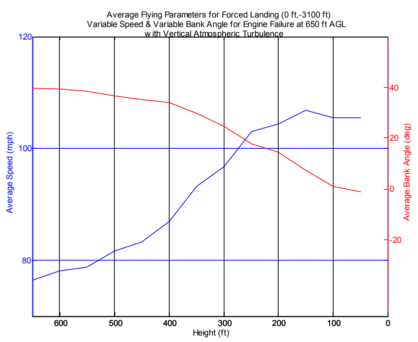

(b)

Fig. 10. Optimal Forced Landing (0 ft, -3100 ft) Continuous Speed and Continuous Bank Angle at 650 ft AGL with Vertical Atmospheric Turbulence

Fig. 11-a shows the best forced landing flight paths with vertical atmospheric turbulence from each of the 100 turbulence profiles for the pre-selected location (3000 ft, 3000 ft). The aeroplane's average flying speed and bank angle at each 50 ft decrement in altitude, and the airplane's final heading statistics to land at the pre-selected location are shown in Fig. 11-b. The effects updrafts have on this landing manoeuvre is a slightly wider flight path or longer flight path since updrafts decrease the descend rate and longer paths are required to bleed off the excess energy (altitude). Flying longer flight paths also have the effect of touching down at the pre-selected location with final headings near the 180º heading relative to the initial engine failure heading.

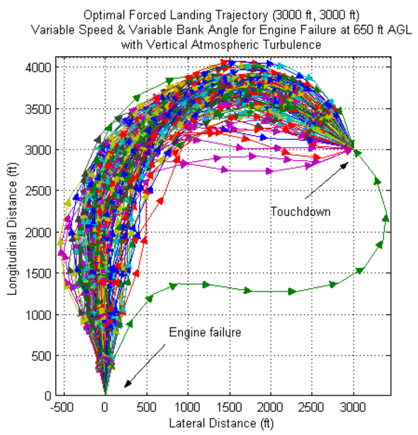

(a)

<u># Runs</u>
<u>Final Heading</u>

6 %
045° ≤ ψ < 090°

51 %
090° ≤ ψ < 135°

42 %
135° ≤ ψ < 180°

1 %
ψ = 310°
(double base leg)

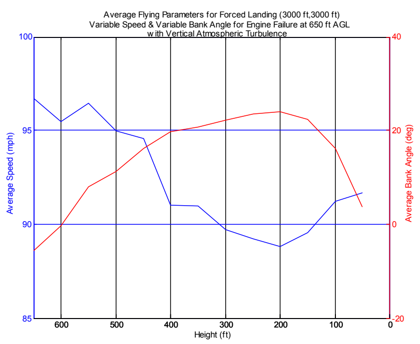

(b)

Fig. 11. Optimal Forced Landing (3000 ft, 3000 ft) Continuous Speed and Continuous Bank Angle at 650 ft AGL with Vertical Atmospheric Turbulence

Fig. 12-a shows the best forced landing flight paths with vertical atmospheric turbulence from each of the 100 turbulence profiles runs and the airplane's final heading statistics for the pre-selected location (500 ft, 200 ft). The aeroplane's average flying speed and bank angle manoeuvres at each 50 ft decrement in altitude to land at the pre-selected location are shown in Fig. 12-b,c. The random vertical disturbances do not seem to affect its performance in landing close to this pre-selected location since vertical disturbances do not affect the turn manoeuvres as much as the straight glide manoeuvres.

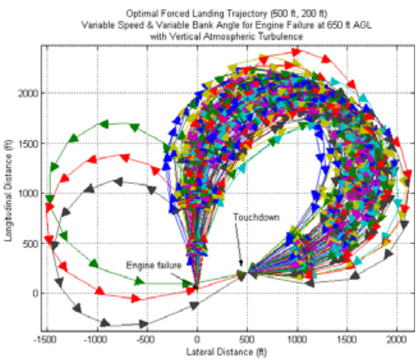

(a)

Runs
Final Heading

3 %
054° ≤ ψ ≤ 076°

97%
220° ≤ ψ ≤ 288°

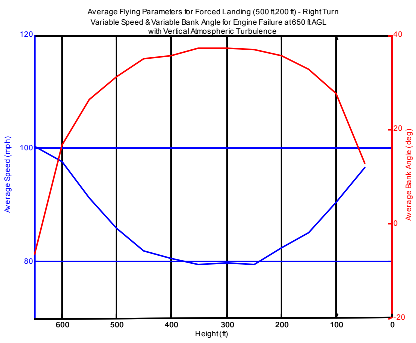

(b)

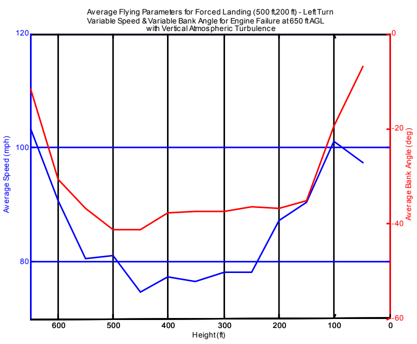

(c)

Fig. 12. Optimal Forced Landing (500 ft, 200 ft) Continuous Speed and Continuous Bank Angle at 650 ft AGL with Vertical Atmospheric Turbulence

6 Discussions

For the test location at (0 ft, -3100 ft), it is intuitive that that are 2 general paths since the pre-selected location lies along the airplane's line of symmetry at engine failure. A double base leg landing can also be clearly seen for the (3000 ft, 3000 ft) location but this flying manoeuvre is not recommended because it is more complicated to fly than the typical base leg to final leg landing manoeuvre and it will also increase the pilot's workload. Statically, GA also found more flying paths for the typical base leg to final leg manoeuvre than for the double base leg landing manoeuvre. Lastly, for the location (500 ft, 200 ft), it is possible to land at the pre-selected location by turning in the opposite direction instead of towards the intended location. This is possible because the pre-selected location is located at close proximity to the airplane's initial line of symmetry at engine failure. It is not recommended to fly this manoeuvre to land at this particular landing location because statistically, GA found more paths in flying the manoeuvre that continuously turn towards the pre-selected location. The lack of gradient information in GA is responsible for its inability to mathematically prove whether the results found are optimum. The trade off in its ability to search a large solution space is the performance sacrifice as a true optimisation procedure.

One of GA's limitations is not being able to locate all the possible trajectories and neither can it guarantee a single best solution since it is a stochastic process based on randomness. In fact, different GA runs may produce different optimal results, possibly more than one unique landing path, perhaps causing uncertainty as to which is the best landing path as can be seen for the pre-selected landing locations tested. GA may also generate results that are intuitive, those may provide more information that would not have been thought of otherwise or results that are counter intuitive as illustrated by the three test locations.

7 Conclusions

The results from various GA search have confirmed GA's effectiveness to explore the solution domain as well as its capability to successfully identify the most promising trajectory paths to a forced landing manoeuvre. The results obtained trace a flight path envelope for the most probable landing flight paths for each of the pre-selected landing location considered, touching down very close to the intended touchdown point on ground. The vertical atmospheric turbulence has the effect of widening the landing path envelope for each of the three locations considered. This is expected since vertical turbulence velocity components effectively changes the vertical descend rate forcing a change in the forced landing manoeuvre to land at the pre-selected landing locations. The vertical disturbances have the most effect on straight glide manoeuvres and are less sensitive to the turning manoeuvres. Overall, the GA procedure developed clearly identified an ensemble of the most promising landing paths within the search domain.

8 References

[1] Rogers, D.F., Possible "Impossible" Turn. *Journal of Aircraft*, Vol. 32, No. 2, pp. 392-397, 1995.

[2] Hoffren, J. and T. Raivio. Optimal Maneuvering After Engine Failure. *AIAA Proceedings of the Atmospheric Flight Mechanics Conference*, Denver, Colorado, AIAA Paper 2000-3992, 2000.

[3] Bramson, A.F., *Glide, flapless and other abnormal landings*. Make Better Landings. Martin Dunitz Ltd, London, 1982.

[4] Trevor Thom, C., *The Forced Landing Without Power*. Private Pilot Flying Training Guide for the Student Pilot. Aviation Theory Centre, 1987.

[5] Tong, P., G. Galanis, and C. Bil, Sensitivity Analysis to a Forced Landing Manoeuvre. *Journal of Aircraft*, Vol. 40, No. 1, pp. 208-210, 2003.

[6] Pamadi, B.N., *Performance, Stability, Dynamics, and Control of Airplanes*. AIAA, 1998.

[7] Anon, *Flying Qualities of Piloted Airplanes*, http://www.aa.washington.edu/courses/aa441/MIL-F-8785.pdf, Military Specifications, Editor. US Department of Defence, 1980.

[8] Newman, D.M. and K.C. Wong, *Six Degree of Freedom Flight Dynamic and Performance Simulation of a Remotely-Piloted Vehicle*. The University of Sydney, Sydney. pp. 22-27, 1993.

[9] Hahn, K.-U., et al. Effect of Wind and Wind Variation on Aircraft Flight - Paths. *AGARDograph No. 301 Aircraft Trajectories Computation - Prediction - Control,* 1990.

[10] Hahn, K.-U., et al. Wind Models for Flight Simulation. *AGARDograph No. 301 Aircraft Trajectories Computation - Prediction - Control,* 1990.

[11] Schanzer, G. Influence of Windshear, Downdraft and Turbulence on Flight Safety. *Agard Conference Proceedings No. 470 - Flight in Adverse Environment Conditions,* 1989.

[12] Holland, J.H., *Adaptation in Natural and Artificial Systems: An introduction Analysis with Applications to Biology, Control, and Artificial Intelligence*. The University of Michigan Press, 1975.

[13] Goldberg, D.E., *Genetic Algorithms in Search, Optimization, and Machine Learning*. Addison-Wesley Publishing Company Inc., 1989.

[14] Michalewicz, Z., *Genetic Algorithms + Data Structure = Evolution Programs*. Springer-Verlag, 1996.

[15] Grefenstette, J.J., Optimization of Control Parameters for Genetic Algorithms. *IEEE Transactions on Systems, Man, and Cybernetics*, Vol. SMC-16, No. 1, pp. 122-128, 1986.

[16] Srinivas, M., Genetic Algorithms: A Survey. *Membership Magazine of the IEEE Computer Society*, Vol., No. June, pp. 17-26, 1994.

[17] Goldberg, D.E., *Optimal Initial Population Size for Binary-Coded Genetic Algorithms*. The Clearing House for Genetic Algorithms, The University of Alabama, Tuscaloosa, Al, Alabama. pp. 1-14, 1985.

[18] Williams, E.A. and W.A. Crossley, Empirically-Derived Population Size and Mutation Rate Guidelines for a Genetic Algorithm with Uniform Crossover, *Soft Computing in Engineering Design and Manufacturing*, P.K. Chawdhry, R.Roy, and R.K. Pant, Editors. Springer-Verlag. pp. 163-172. 1998.